Acadlore Transactions on AI and Machine Learning
https://www.acadlore.com/journals/ATAIML

Adaptive Lane Keeping Assistance System with Integrated Driver Intent and Lane Departure Warning

Haigang Wei[1], Wei Tong[2], Yueyong Jiang[3], Jianlu Li[2*], Ramesh Vatambeti[4]

[1] GAC MOTOR Co., Ltd., 511434 Guangzhou, China
[2] Technology Center of GAC MOTOR Co., Ltd., 511434 Guangzhou, China
[3] College of Automotive Engineering, Jilin University, 130022 Changchun, China
[4] School of Computer Science and Engineering, VIT-AP University, 522237 Vijayawada, India

[*] Correspondence: Jianlu Li (lijianl@gacmotor.com)

Received: 10-22-2023 **Revised:** 12-27-2023 **Accepted:** 01-12-2024

Citation: H. G. Wei, W. Tong, Y. Y. Jiang, J. L. Li, and R. Vatambeti, "Adaptive lane keeping assistance system with integrated driver intent and lane departure warning," *Acadlore Trans. Mach. Learn.*, vol. 3, no. 1, pp. 11–23, 2024. https://doi.org/10.56578/ataiml030102.

Abstract: The development of an adaptive Lane Keeping Assistance System (LKAS) is presented, focusing on enhancing vehicular lateral stability and alleviating driver workload. Traditional LKAS with static parameters struggle to accommodate varying driver behaviors. Addressing this challenge, the proposed system integrates adaptive driver characteristics, aligning with individual driving habits and intentions. A novel lane departure decision model is introduced, employing time-space domain fusion to effectively discern driver's lane change intentions, thus informing system decisions. Further innovation is realized through the application of reinforcement learning theory, culminating in the creation of a master controller for lane departure intervention. This controller dynamically adjusts to driver behavior, optimizing lane keeping accuracy. Extensive simulations, coupled with hardware-in-the-loop experiments using a driving simulator, substantiate the system's efficacy, demonstrating marked improvements in lane keeping precision. These advancements position the system as a significant contribution to the field of driver assistance technologies.

Keywords: Adaptive lane keeping assistance system; Reinforcement learning; Lane departure intervention; Driver behavioral analysis

1 Introduction

In the context of burgeoning economic globalization and rapid urbanization, an escalation in vehicle numbers has been observed, leading to increasingly intricate urban road networks and exacerbated traffic issues. Predominantly, lane departure incidents constitute a significant portion of vehicular accidents. Such occurrences not only lead to collisions between vehicles in longitudinal traffic but also pose a risk of rollovers during lane changes, especially for larger vehicles, underscoring the criticality of effective lane-keeping for vehicular safety. Recent years have seen a surge in the development of Advanced Driver Assistance System (ADAS), a pivotal component of which encompasses vehicle lateral driving assistance systems. This domain has evolved to include various forms, notably Lane Departure Warning (LDW) and LKAS. The design of LKAS, particularly concerning control methodologies, encounters two principal challenges. Firstly, the simplification of the nonlinear characteristics of driver and vehicle dynamics models through linearization results in substantial predictive inaccuracies, impeding the attainment of optimal control. Secondly, the inherent uncertainties in traffic environments, vehicle parameters, and driver behaviors necessitate a robustness in model-based controllers to maintain stability under varying conditions. Addressing these challenges, a myriad of classical control algorithms has been integrated into LKAS controller design. These include state feedback control [1], H2 predictive optimal control [2], optimal control [3], and MPC [4]. Furthermore, to manage the nonlinearities of the control subjects, sliding mode control methodologies [5] have been employed. To overcome the second challenge, the principles of Liapunov's equation, $H\infty$ control [6], and self-correcting regulators [7] have been widely adopted in auxiliary controller design, ensuring robust performance amidst uncertainties.

Amidst the escalating prominence of artificial intelligence (AI), deep learning and reinforcement learning have emerged as pivotal forces steering the trajectory of AI development, profoundly impacting various aspects of daily

life. The integration of these technologies into lane keeping strategies has been the focus of recent scholarly efforts. An Recurrent Neural Network (RNN) retention system, utilizing long- and short-term memory units, was proposed by Jeong [8]. This system was trained using a dataset derived from three drivers, indicating a tailored approach to learning driver behavior. Concurrently, Basjaruddin et al. [9] introduced a sensor fusion system for lane keeping, highlighting the integration of multiple data sources for enhanced system performance. In the realm of reinforcement learning, El Sallab et al. [10] delineated two algorithm categories: discrete and continuous actions, both demonstrating improvements in accuracy for lane keeping applications. Luo et al. [11] embarked on an investigation concerning lane keeping in scenarios characterized by saturated data volumes, a study signifying the challenges posed by data-intensive environments. Further, Wang et al. [12] substantiated the effectiveness of Deep Q-Network (DQN) and Deep Deterministic Policy Gradient (DDPG) algorithms in maintaining lane integrity, thereby affirming their applicability in this domain. Kim et al. [13] innovatively proposed a convolutional hybrid density model, specifically tailored for lane keeping strategies, indicating a novel approach in this field.

In the domain of driver behavior analysis, Yang et al. [14] from Jilin University utilized Support Vector Machine (SVM), employing vehicle longitudinal velocity, the relative distance between vehicles, and longitudinal acceleration as state quantities. This approach, incorporating a polynomial kernel function, effectively categorized outputs into lane change decisions, underscoring the accuracy of SVM in discerning deliberate lane changes. Wang and Du [15] of Hunan University developed a hybrid model combining Hidden Markov Model (HMM) and SVM. By using steering wheel angle and accelerator pedal data as observational variables, the model demonstrated a marked improvement in accuracy and real-time performance over singular SVM or HMM algorithms. This model could predict lane change intentions approximately 1.3 seconds before the actual maneuver, a significant advancement in predictive analytics. Despite its high accuracy and real-time capabilities, the network exhibited susceptibility to errors in the presence of sample noise, occasionally leading to non-convergence and network failure.

Despite extensive research and development in LKAS, a notable gap persists in their environmental perception and analysis of driver characteristics [16]. This study aims to bridge this gap by delving into the driving characteristics of individuals, thereby addressing the limitations inherent in LKAS with static parameters, which are less effective for drivers with diverse driving habits. To confront these challenges, a driving simulation platform is employed to construct a simulation experiment scenario. Within this framework, data pertaining to the driver's lateral offset and Time to Lane Crossing (TLC) values at the steering return point during lane keeping are meticulously collected. Subsequently, a lane keeping controller based on the DDPG algorithm is developed. This controller selects lateral offset and relative yaw angle as key indicators to constitute the state space for DDPG [17] training, focusing on deviation states.

The study's primary contributions are twofold: Firstly, it presents a modified TLC algorithm that innovatively integrates time and space domains in the context of lane departure decision-making. Secondly, it proposes an assisted intervention algorithm that synergizes driver intent with lane departure decisions. These advancements represent a significant stride in enhancing the adaptability and efficacy of LKAS, tailoring it to accommodate individual driver characteristics and environmental variables.

2 Method

This section delineates the methodology employed to examine the assistance form of the LKAS, encompassing driver behavior habits, and the recognition and control of driver lane change intentions. An algorithmic flowchart, illustrated in Figure 1, elucidates the proposed methodology.

In Figure 1, the core component is an LSTM-based model, meticulously developed for the recognition of driver intentions. This model is designed to precisely discern the driver's intent during vehicle operation. In instances where the driver exhibits no explicit intention to change lanes, yet the vehicle is at risk of deviating from its current lane, an alert mechanism is activated. Concurrently, the controller initiates an intervention to aid in the maintenance of the vehicle's lateral position. During the intervention phase, a critical evaluation occurs in each cycle prior to determining the output control measure, specifically the front wheel angle. This evaluation entails assessing whether the driver is actively engaged in controlling the vehicle. Should the assessment reveal that the driver is consciously directing the vehicle, the controller ceases its intervention, thereby ensuring the driver's paramount control over the vehicle. Additionally, the intervention is terminated if the vehicle reaches a state of safety.

Contrasting with conventional neural networks, RNNs exhibit a distinctive feature where interconnections between nodes in hidden layers are present [18]. The input for a hidden layer at a given moment comprises not only the current input but also the output from the hidden layer at the preceding time point. This structure enables RNNs to extract relevant features within a sequence, thereby unveiling relationships within the data. The fundamental unit of an RNN is an array of infinite RNN units [19]. While RNNs adeptly handle time-related challenges, their ability to retain the weight of prior state information diminishes over time, potentially becoming negligible. This fading of early information, crucial for certain problems, is inadequately preserved in the RNN structure. To mitigate this limitation, Long Short-Term Memory (LSTM) networks have been proposed by scholars. In contrast to RNNs, LSTMs possess

the capability to store time series features within their parameters [20], effectively retaining parameters with larger gradients.

In pursuit of authentic and diverse driving data, the present study utilizes the simulation software VI-grade. This software simulates a common three-lane scenario, with each lane measuring 3.75 meters in width, and incorporates additional traffic elements like traffic lights. The data harvested encompasses vehicle motion status, environmental data, and driver operation behavior. Utilizing VI-grade's built-in dynamics model, vital information such as the vehicle's center of mass position, heading angle, speed, and steering wheel angle are directly obtained. The initial step involves analyzing the differences between vehicle motion parameters and driver operations during lane change and lane-keeping processes using the collected posture data. Subsequently, parameters that broadly represent the driver's lane change patterns are selected as observational variables for LSTM. Relevant data series are filtered, forming the training set. The network structure is then trained, and its accuracy is further enhanced by 4% through the application of SVM [21].

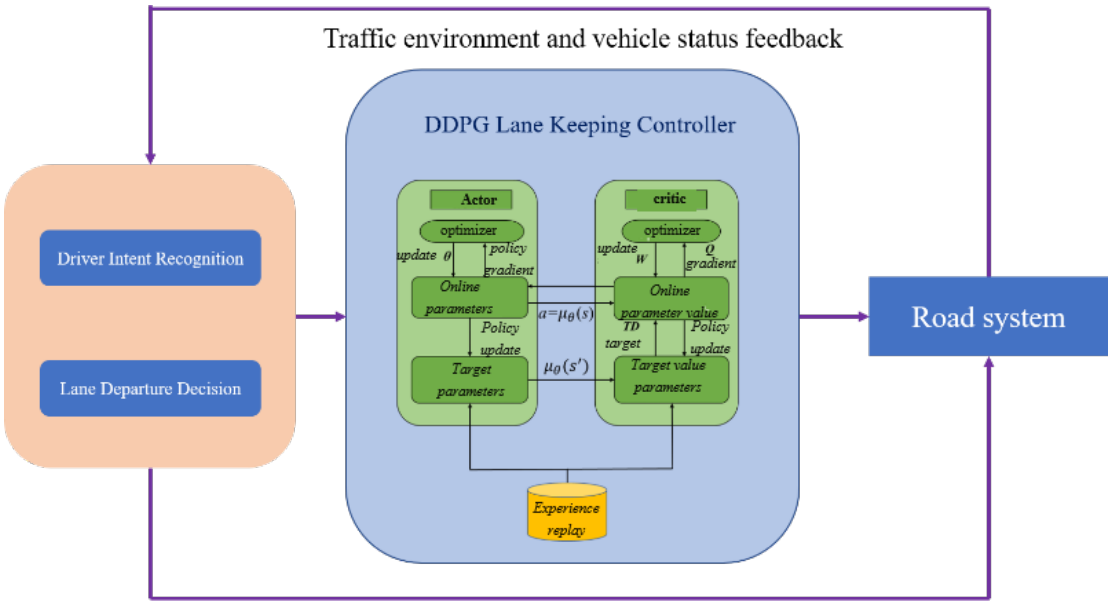

Figure 1. Algorithm flowchart

2.1 Fusion of Time Domain and Space Domain in TLC Lane Departure Algorithm

In this subsection, a lane departure decision-making model is introduced, synthesizing both temporal and spatial domains. This model is predicated on defining a safe driving area within a lane, contingent upon the driver's habitual control of the lateral position during lane-keeping.

Initially, the safe driving area within the lane, where the vehicle currently resides, is delineated (Figure 2). The safe driving area's left boundary's relative distance to the lane's centerline is denoted by y_{left} , whereas y_{right} represents the distance to the right boundary, and b_c signifies the lane width.

In the spatial domain, the left and right boundaries of the safe driving area are $y_{left} = \min\left(\frac{b_c}{2} - y_d, y_{el} + \frac{b}{2}\right)$ and $\max\left(-\frac{b_c}{2} + y_d, y_{er} - \frac{b}{2}\right)$, respectively. Here, y_d is defined as the cumulative 95% lateral offset of the vehicle's center of mass during lane keeping, whereas y_{er} corresponds to the cumulative 5% lateral offset.

The safe area is mathematically represented as follows:

$$\mathrm{U} \in \left\{ y^*_{\text{left}} \leq y_{\text{left}} \text{ and } y^*_{\text{right}} \leq y_{\text{right}} \right\} \tag{1}$$

where, y^*_{left} and y^*_{right} are the thresholds delineating the current safe driving area.

This segment addresses the dynamics involved when a vehicle deviates from its lane, focusing on the driver's reaction time and the steering actuator's response. The driver's reaction time, denoted as t_2, is the interval required for the driver to initiate corrective measures upon deviation detection. Additionally, due to the inherent delay in the steering actuator, a response time, represented by t_3, ensues before the front wheels adjust their angle in response to the driver's actions. It is posited that if "TLC" a exceeds a certain threshold of $t_1 + t_2 + t_3$, lane departure becomes inevitable. Furthermore, the model incorporates the driver's steering habits and the vehicle's dynamic steering limits

by setting a TLC dynamic threshold.

$$T_{\text{th}} = \max\left(T_s, t_1 + t_2 + t_3\right) \tag{2}$$

This threshold is defined as the duration required for the vehicle to move parallel to the lane line at its maximum yaw rate, denoted as t_1. In summary, the lane departure decision model's principle is illustrated in a flowchart, as shown in Figure 3.

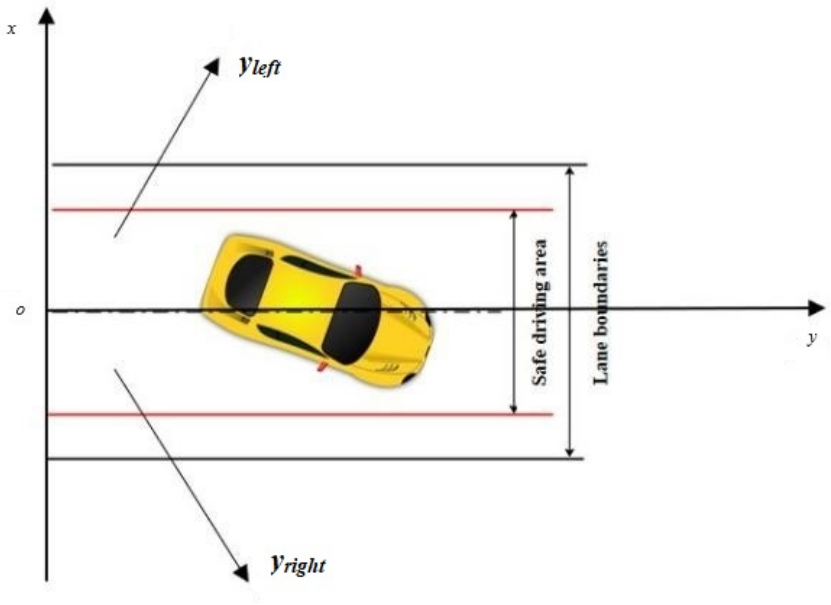

Figure 2. Schematic diagram of the safe driving area

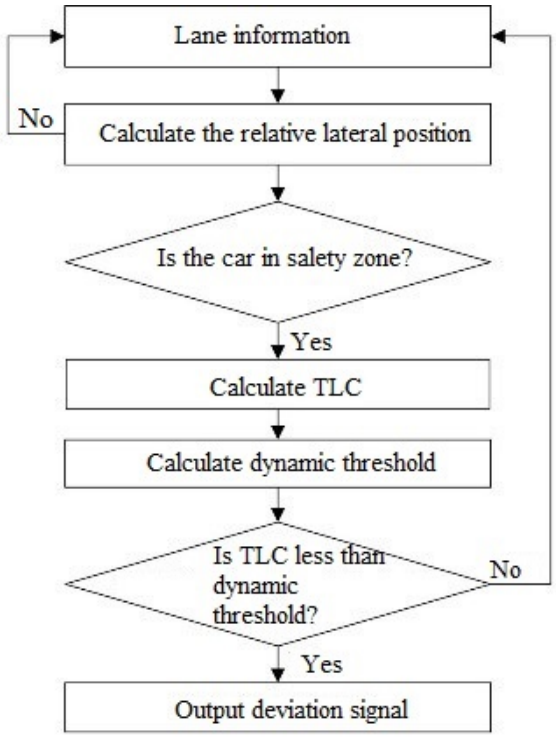

Figure 3. Flowchart of the lane departure decision model

2.2 Application of a Reinforcement Learning Algorithm in the Intervention System

The study integrates reinforcement learning into the intervention system, where the agent, through a process of "trial and error," refines its behavior based on rewards gained from environmental interactions. The objective is the maximization of cumulative rewards. Unlike direct action generation, reinforcement learning evaluates and provides feedback on the agent's actions based on environmental rewards. Owing to limited external environmental information, the agent relies solely on its experiences for learning. The reinforcement learning system progressively refines its behavior to better adapt to the environment, guided by action evaluations.

In comparison with the DQN algorithm, the DDPG algorithm is more suited for continuous tasks, such as those required in a LKAS. The state space is conceptualized as a representation of the agent's external environment. An effective state space should encapsulate the vehicle's current position and deviation with minimal observational variables. In this study, the state space comprises two variables: lateral offset and relative yaw angle. Figure 4 illustrates the generation of the state space for the DDPG algorithm.

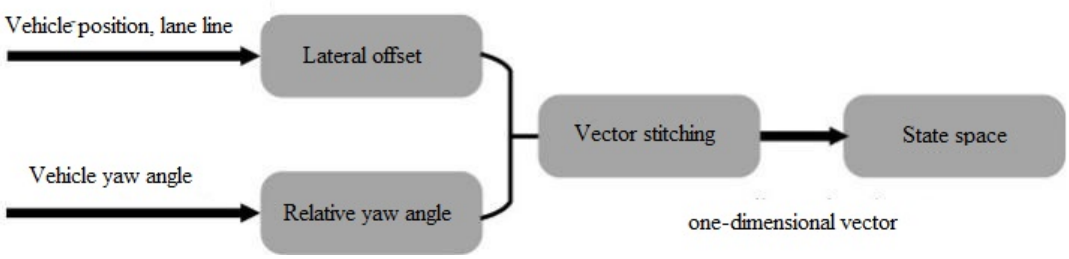

Figure 4. State space generation of DDPG

The study takes into consideration the practical aspects of vehicle steering control, adopting the front wheel angle as the action output. Given that the vehicle's front wheel angle constitutes a continuous action space, the DDPG algorithm is capable of generating continuous control actions. This capability facilitates the attainment of more stable lateral vehicle motion. Consequently, the front wheel rotation angle is selected as the reinforcement learning action value.

In the domain of reinforcement learning, the formulation of the reward function is pivotal for the agent's acquisition of an optimal policy. An aptly designed reward function enables the agent to derive a reasonable policy. This reward function must encapsulate both safety and comfort aspects to facilitate the learning of an effective lane-keeping policy.

(a) Safety factors

The primary objective of the lane-keeping controller is to ensure the vehicle remains within its original lane. Therefore, the first safety criterion involves assessing whether the vehicle deviates from its designated lane. A state quantity is designated to represent c_t. Here, c_t=1 signifies a deviation from the original lane, while c_t=0 indicates adherence to the lane. In instances of c_t=1, a negative reward is assigned to the agent as a penalty.

(b) Comfort factor

Passenger comfort is compromised when the vehicle experiences significant jolts due to large increments in the front wheel angle. To address this, a penalty term is integrated into the reward function. The comfort parameter ε is utilized to penalize the jitter phenomenon if $(a_{t+1} - a_t) > \varepsilon$, applying the sigmoid function for mapping the penalty value, as outlined in Eq. (3).

$$p = \begin{cases} 0, & a_{t+1} - a_t \geq \varepsilon \\ \frac{1}{1+e^{\cos \varepsilon}}, & a_{t+1} - a_t < \varepsilon \end{cases} \tag{3}$$

The parameters within the reward function necessitate continuous adjustments and training to attain the desired outcomes. The final formulation of the reward function is represented as follows:

$$R_t = -5.0\left(o_t^2 + 2s_t^2\right) - 10abs\left(\delta_f\right) - 5.0\left(\dot{o}_t^2 + \dot{s}_t^2\right) - 100c_t - p \tag{4}$$

where, R_t denotes the reward at time t, O_t and S_t represent the lateral offset and relative transverse sway angle of the vehicle at time t, respectively, and δ_f indicates the front wheel rotation angle at time t.

In the training of the DDPG algorithm, critical parameters are meticulously set, as delineated in Table 1.

Prior to each training iteration, the initial state of the vehicle is configured as specified in Eq. (5).

$$\mathrm{y}_e = \mathrm{rand}(-1, 1); \varphi = \mathrm{rand}(-0.2, 0.2) \tag{5}$$

Table 1. Hyperparameter settings for DDPG

Parameters	Description	Value
Optimizer	Optimization	Adam
Discount factor	Discount rate for cumulative returns	0.9
Value network learning rate	Value network update step size	0.001
Policy network learning rate	Policy network update step size	0.001
Batch size	The number of samples in a batch gradient descent	64
Experience pool size	For sample storage	2000

Figure 5 depicts the training process rewards of the DDPG algorithm after 20,000 training rounds. The graph presents two curves representing the cumulative reward and the average reward per round during the training phase.

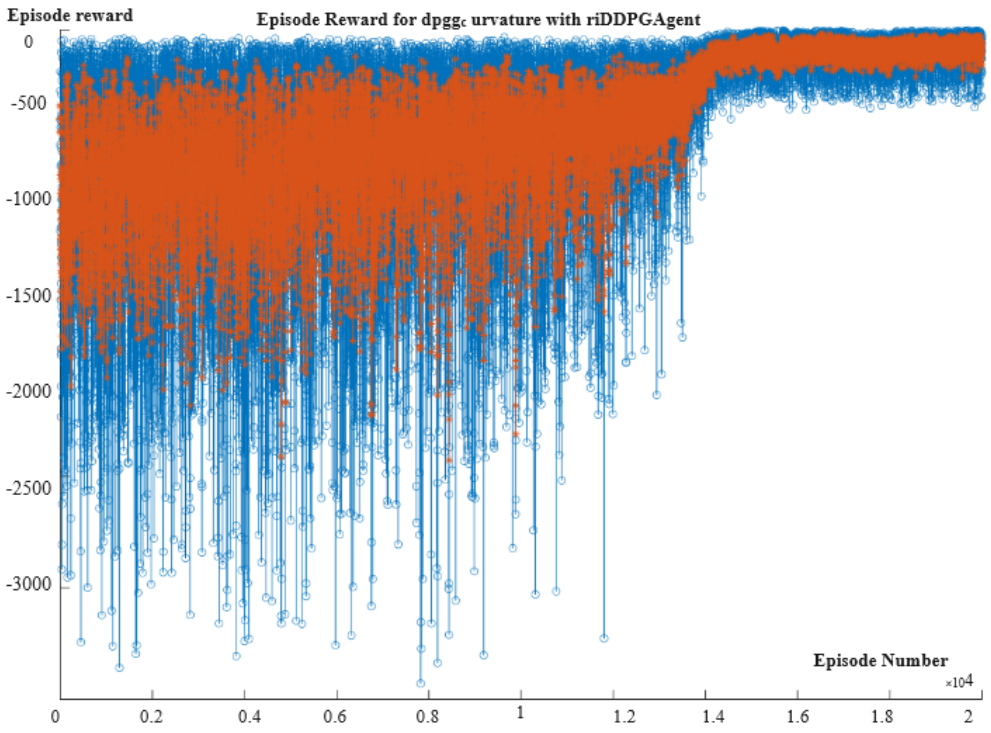

Figure 5. Training process rewards

The convergence of the DDPG algorithm is evident after approximately 14,000 rounds of environmental interaction, indicating successful strategy learning. Across varying observational states, the algorithm demonstrates a continuous improvement in its control strategies, enhancing its performance in the lane-keeping task. Notably, the cumulative payoff exhibits a potential for further increase with the progression of training rounds.

3 Result

3.1 Simulation Test

Simulation tests were conducted under three distinct conditions: straight lane, curved lane, and double shift lane, to assess the proposed algorithm's efficacy in maintaining the vehicle within its original lane. For the straight lane condition, the initial parameters were set as follows: the vehicle's initial lateral position deviation was 0.8 m, and the relative yaw angle was 0.05 rad. The lane width was determined to be 3.75 m, the vehicle width 2 m, and the adhesion coefficient 0.8. Vehicle speeds were configured at 15 and 25 m/s, with the simulation lasting for 10 seconds. The outcomes for the straight lane condition are depicted in Figure 6.

In subgraph (a) of Figure 6, it is observed that with a consistent initial yaw angle, an increase in vehicle speed results in greater vehicular inertia, leading to continued deviation to the left. In comparison with the Model Predictive Control (MPC) controller, the lateral position deviation managed by the DDPG agent remains similar during the process of controlling the vehicle's lateral position. As demonstrated in subgraph (b) of Figure 6, in the initial stages, the DDPG agent induces a significant rightward front wheel angle to correct the heading angle deviation, thereby facilitating a positive vehicle direction and mitigating further deviation. Subgraphs (c), (d), (e) and (f) of Figure 6

reveal that at lower speeds, the front wheel angle adjustments are comparatively smoother, and the resultant lateral acceleration is relatively minimal.

In the simulation of curved road conditions, the initial lateral offset and relative yaw angle were set at 0, with the curvature of the curve established at 0.002. Vehicle speeds were simulated at 15 and 25 m/s, with a road adhesion coefficient of 0.8. The performance of the DDPG agent was compared against the widely used MPC algorithm, as illustrated in Figure 7.

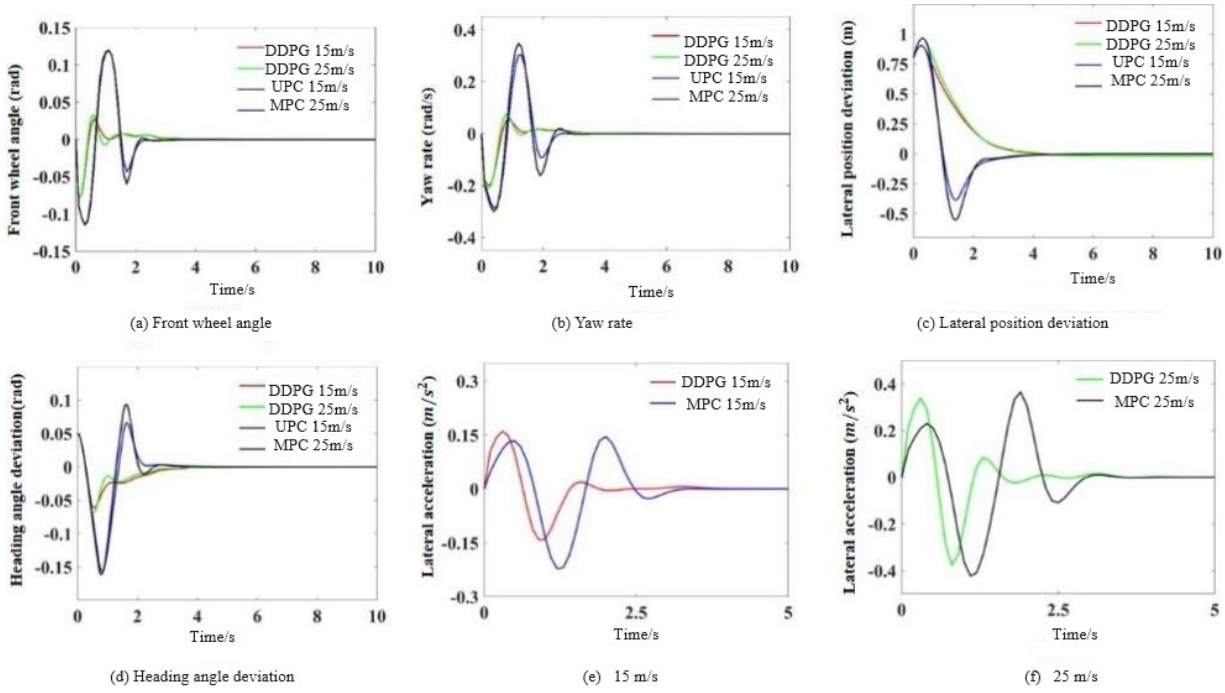

Figure 6. Simulation results for straight road conditions

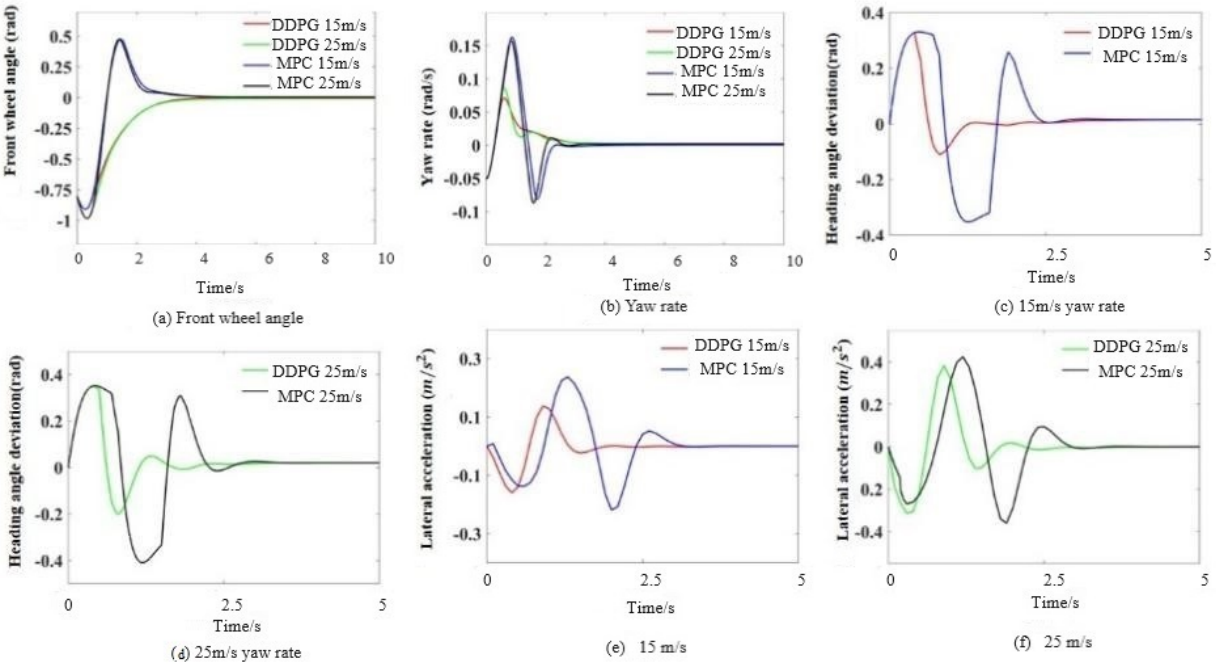

Figure 7. Simulation results

The simulation results indicate that the DDPG agent maintains robust lane-keeping capabilities on curved roads,

analogous to its performance on straight roads. The agent effectively corrects vehicle deviation, ensuring optimal vehicle posture and stability throughout the process, which spans approximately 4 seconds.

For the double line shifting scenario, the initial conditions were set with both lateral offset and relative yaw angle at 0. The vehicle speeds for simulation were again 15 and 25 m/s. Figure 8 depicts the follow-up results for the double line-moving conditions.

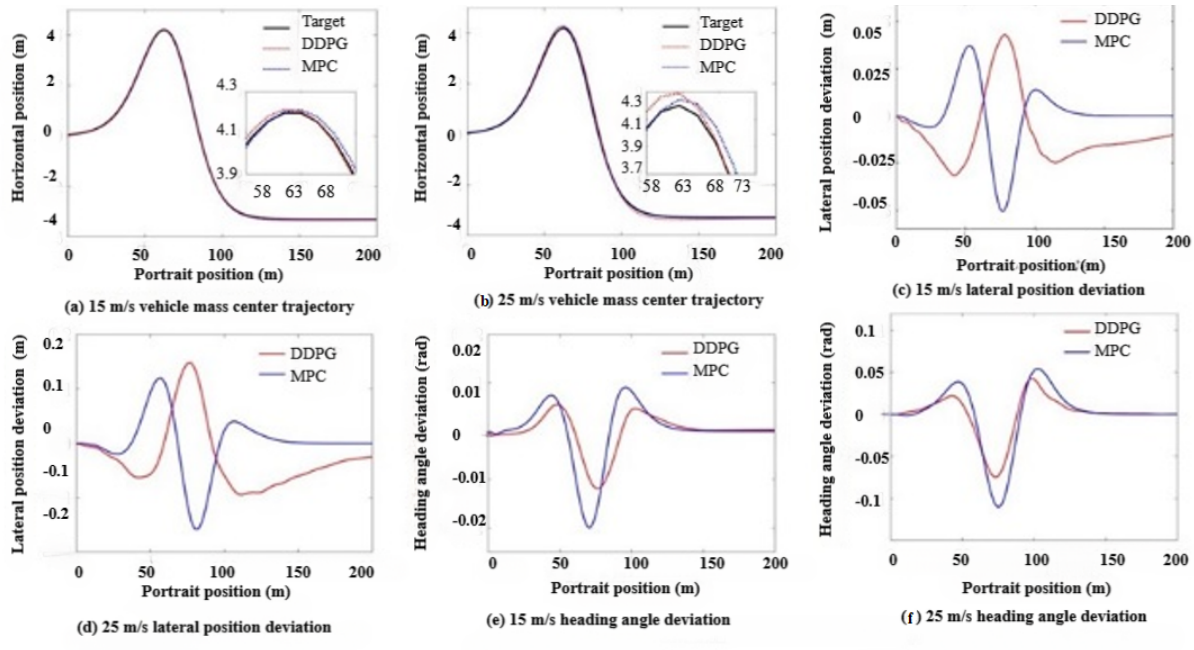

Figure 8. Follow-up results for the double line-moving conditions

The performance of the DDPG agent under double line-shifting conditions, as depicted in Figure 9, demonstrates its proficiency in adhering to the path, particularly in segments with less pronounced curvature. The trajectory followed by the DDPG agent aligns closely with the target trajectory, except in areas of high curvature. A distinct contrast is observed in the control strategy of the DDPG agent when compared to the MPC controller for the same operational conditions.

To further evaluate the DDPG agent's capability in correcting lane departures, a scenario with the vehicle deviating to the left was simulated. The initial lateral offset and relative yaw angle were set at 0.8 m and 0.05 rad, respectively. The simulation outcomes are presented in Figure 9.

The road curvature in the double-line shifting scenario is dynamic, significantly impacting both the lateral position deviation and the heading angle deviation as managed by the controller.

3.2 Simulation Experiment Platform and Experiment Scene Design

The dynamic driving simulator constitutes the core of the simulation hardware platform utilized in this study. This platform integrates various components: the driving simulator itself, a control module, scene simulation, and a vehicle dynamics system.

Employed in the driving simulator are actual vehicle components such as the steering wheel, accelerator pedal, and instrument panel, alongside various actuator components. These elements collectively simulate a realistic driving environment. An operation feedback system is incorporated, allowing the driver to experience the reactive forces from the actuators during maneuvers like acceleration and steering. This system significantly enhances the driver's experiential realism.

Within the simulation platform, VI-grade software not only furnishes road scenarios but also encompasses a vehicle dynamics model. This model facilitates direct acquisition of crucial data inputs from the driver, such as vehicle speed, position coordinates, and steering wheel angle. The integration of VI-grade into the platform obviates the need for extensive communication between different software during simulations, thereby streamlining the simulation process. The software interfaces with the Simulink controller and the assist system's sub-modules through S-functions, ensuring efficient integration and functionality.

3.2.1 Functional integration verification

To validate the functional integration of the lane keeping assist system, the steering wheel angle and rotation speed were set to 0, simulating a scenario where the driver is not actively involved in the driving process [-1.6, 1.5].

Additionally, a safe interval of 0.6 was established to ascertain whether the system could appropriately intervene and disengage based on the lane departure decision model's deviation signal and the driver intention recognition module's judgment. The simulation results under curved road conditions are presented in Figure 10 and Figure 11.

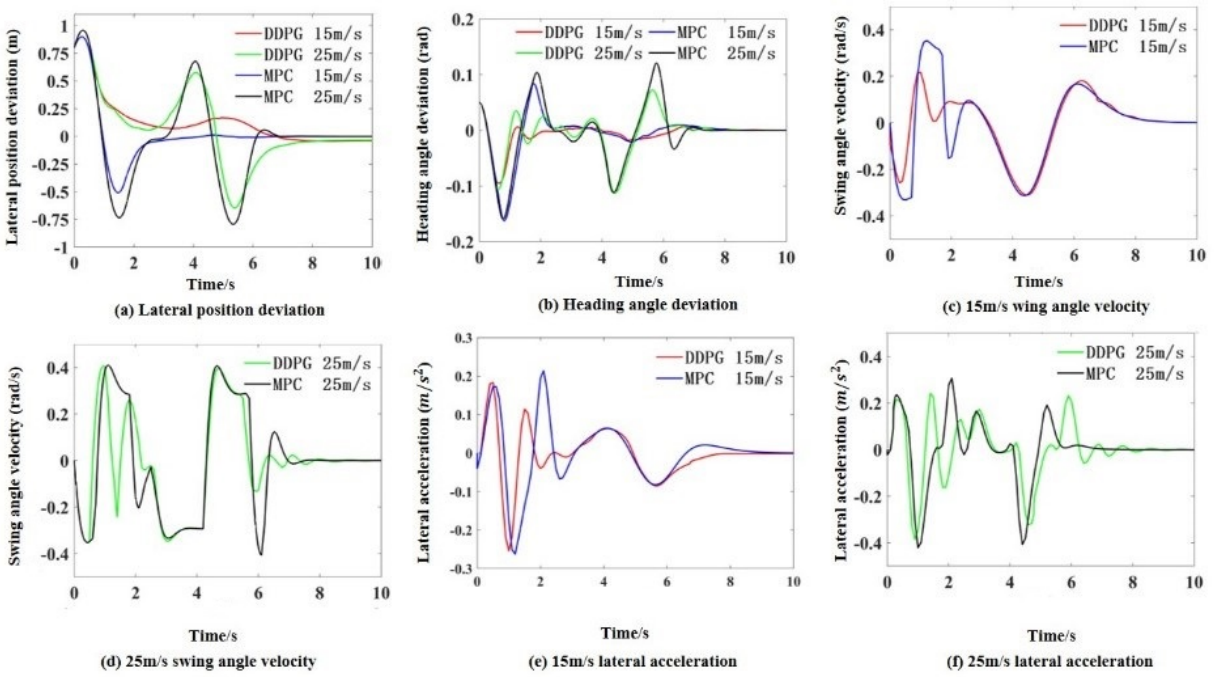

Figure 9. Simulation results of deviation correction for double line shifting conditions

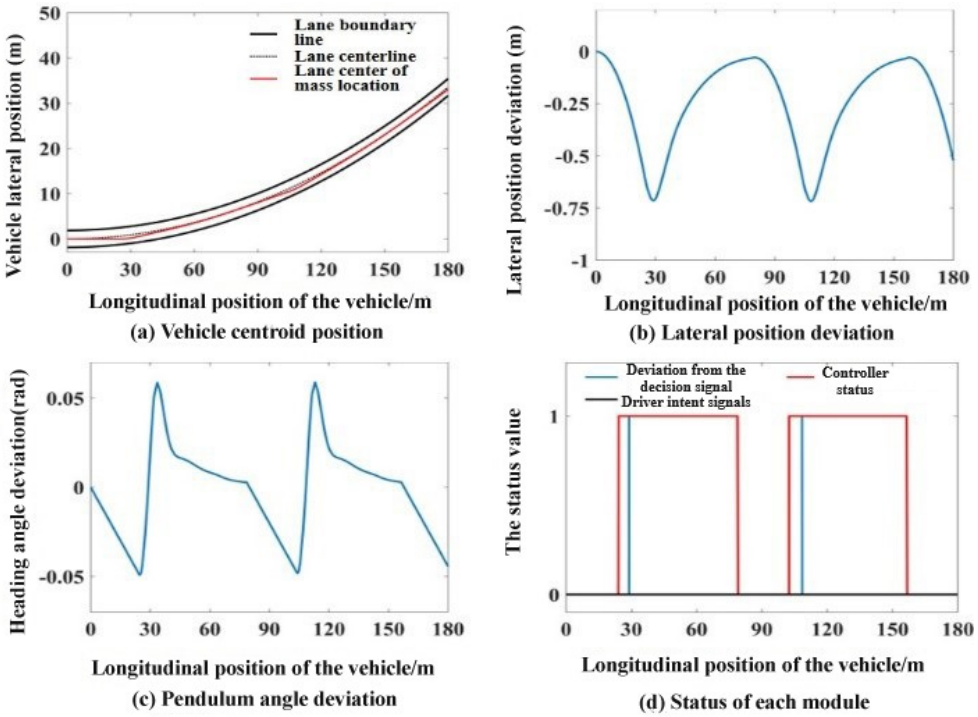

Figure 10. Simulation results for deviation correction in double line-shifting conditions

The system's comprehensive performance was also assessed under sinusoidal conditions to further examine its adaptability to complex operational environments. The initial settings mirrored those of the double lane-shifting scenarios, and the simulation duration was extended to 20 seconds. The results of this simulation are depicted in Figure 12. The simulation results demonstrate the effectiveness of the proposed deviation intervention LKAS. It was

observed that the system intervenes aptly based on the lane departure decision model's output and the driver intention recognition module's analysis. Upon detecting the vehicle's return to a safe state, the system appropriately disengages from the intervention.

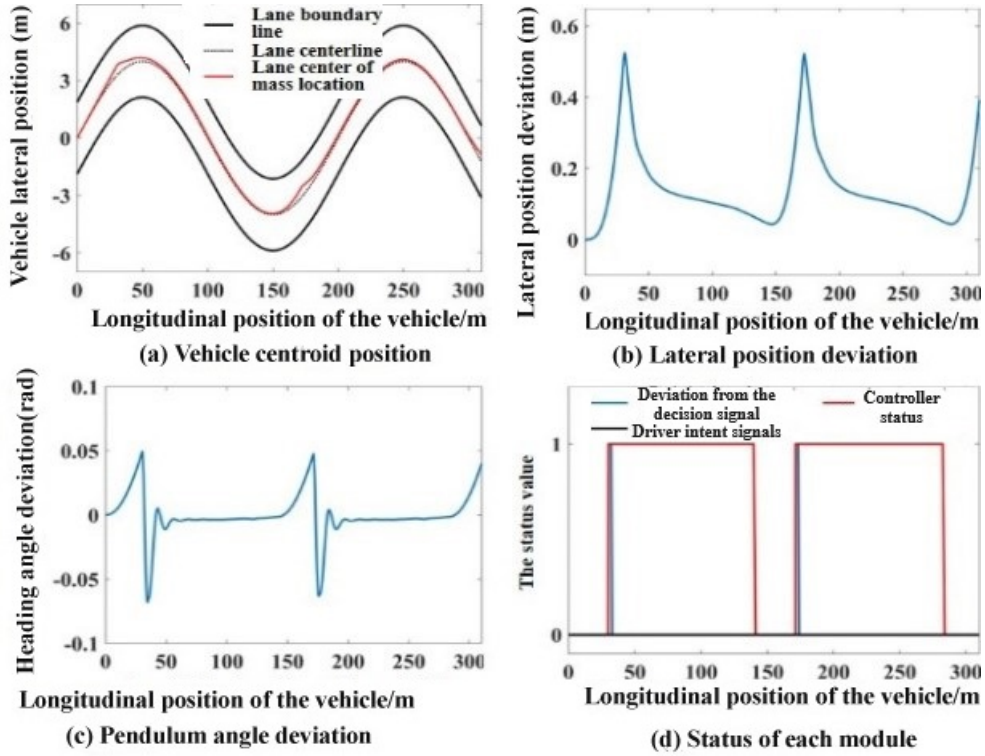

Figure 11. Simulation outcomes under double line shift conditions

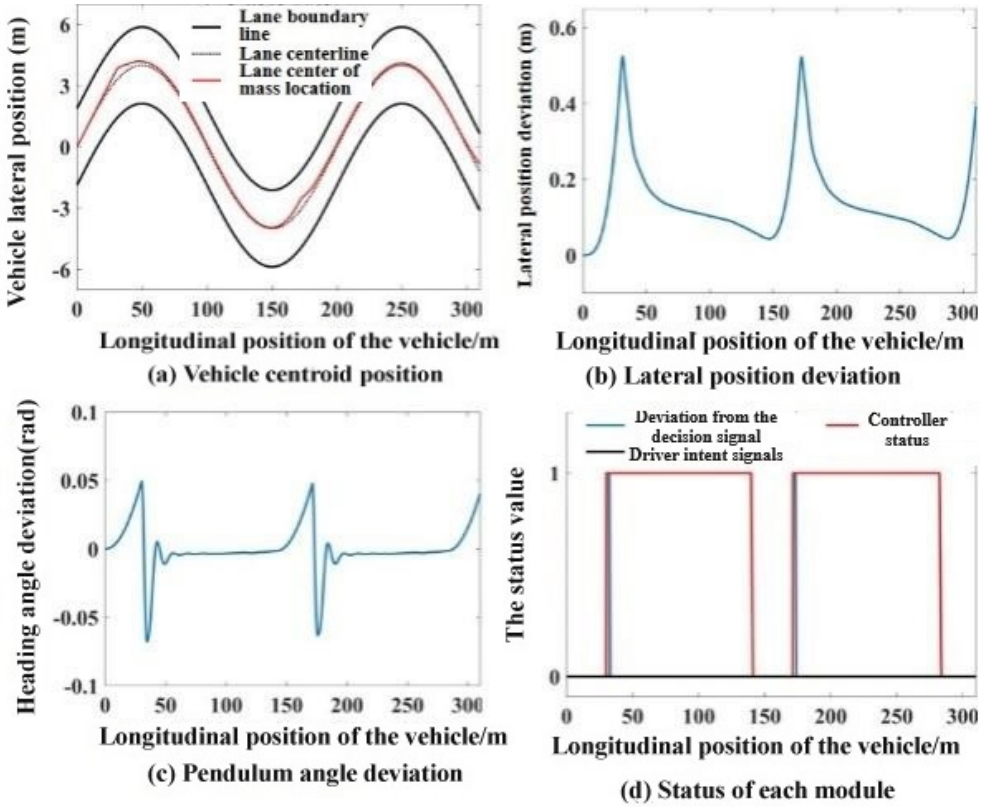

Figure 12. Sinusoidal condition simulation results

In subgraph (a) of Figure 13, the vehicle's center of mass offset relative to the lane centerline is displayed. A positive offset signifies a deviation to the left of the centerline, while a negative offset indicates a shift to the right. Regarding lane positioning, values are assigned as follows: 1 for the left lane, 0 for the middle lane, and -1 for the right lane. Subgraph (b) of Figure 13 illustrates the driver intent identification, where 1 indicates an intent to change lanes to the left, 0 to maintain the current lane, and -1 for a lane change to the right. The deviation decision signal is also represented, with 1 indicating a system prediction of lane departure and 0 suggesting no immediate danger of deviation. Subgraph (c) of Figure 13 shows the steering wheel rotation angle and speed as input by the driver. The DDPG intelligent agent, trained in this study, has effectively completed the lane-keeping task. The lane departure decision model and the driver intention recognition module have accurately identified the driver's intentions and the current deviation status.

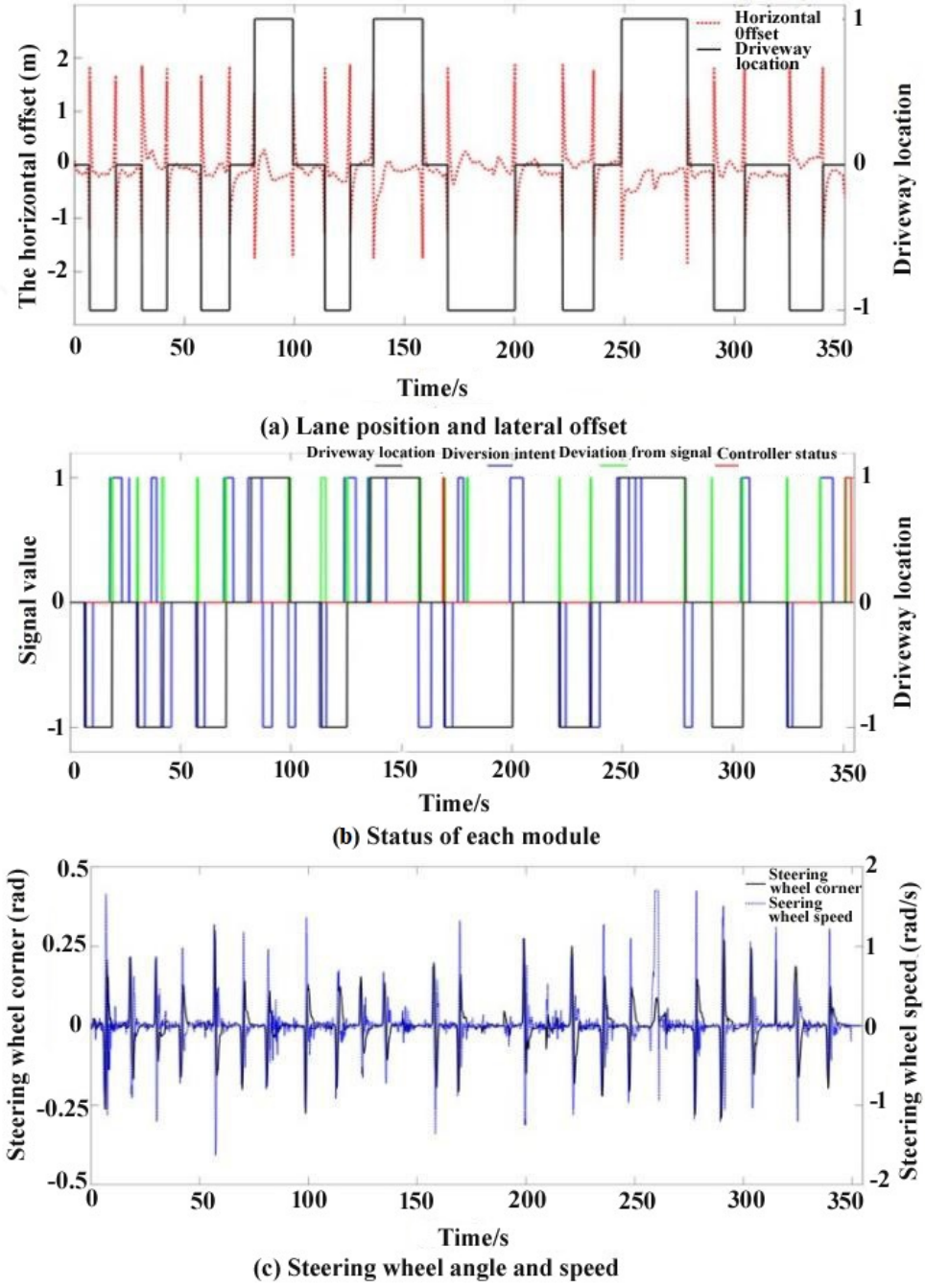

Figure 13. Driver-in-the-Loop simulation results

3.2.2 Future prospects

Effective lane-keeping systems significantly contribute to road safety by preventing vehicular deviation and collisions. These systems enhance driving safety through real-time monitoring of the vehicle's surroundings and implementing pertinent control measures.

Furthermore, lane-keeping strategies are integral to the advancement of autonomous driving technologies. The continuous refinement of lane-keeping systems augments the reliability and safety of autonomous driving systems, thus forming a cornerstone for the future evolution of this technology.

Future developments in lane-keeping systems will focus on more comprehensive integration with other vehicular systems, such as navigation and adaptive cruise control, to facilitate more advanced driving assistance. The incorporation of AI technologies, including deep learning, will enable these systems to more adeptly recognize obstacles like lane markings, other vehicles, and pedestrians. This will lead to the adoption of more sophisticated decision-making and control strategies, further enhancing driving safety.

4 Conclusions

In the rapidly evolving automotive industry, heightened intelligence is a key trend, with ADAS gaining prominence for their contribution to enhancing the driving experience. This study established a lane departure decision-making model that integrates safe driving intervals and latest warning times, considering both temporal and spatial dimensions. The efficacy of this algorithm was validated through simulations of various deviation scenarios, demonstrating a significant reduction in misjudgment rates compared to traditional fixed-threshold lane departure algorithms. The methodology involved analyzing differences between vehicle motion parameters and driver operations during lane change and lane keeping. Key parameters reflecting general lane change patterns were selected as observational variables for the LSTM network. After screening the relevant data series, a training set was constructed, and the network structure was trained, achieving a 4% improvement in accuracy over the SVM.

Furthermore, this study innovatively fused lane departure decision and driving intention recognition algorithms, verifying the effectiveness of this combined approach. A lane-keeping controller was developed using the DDPG algorithm, selecting lateral offset and relative yaw angle as state space components. The front wheel turning angle was utilized as the control quantity, reflecting practical vehicle control scenarios. The design of the reward function focused on achieving driving safety, comfort, and minimizing jitter during lateral motion. Experimental results indicate that the system effectively manages lateral position deviation without overshoot, and course angle deviation is minimized, resulting in less lateral acceleration, smoother processes, and enhanced comfort compared to the MPC algorithm across straight, curved, and double-shift conditions.

Data Availability

The data used to support the research findings are available from the corresponding author upon request.

Conflicts of Interest

The authors declare no conflict of interest.

References

[1] J. Kim, S. Lee, S. Shin, and S. Jeong, "Development of active lane keeping assist system," in *SAE 2013 World Congress & Exhibition*, 2013. https://doi.org/10.4271/2013-01-0718

[2] L. Saleh, P. Chevrel, F. Claveau, J. F. Lafay, and F. Mars, "Shared steering control between a driver and an automation: Stability in the presence of driver behavior uncertainty," *IEEE Trans. Intell. Transp. Syst.*, vol. 14, no. 2, pp. 974–983, 2013. https://doi.org/10.1109/TITS.2013.2248363

[3] C. Sentouh, B. Soualmi, J. C. Popieul, and S. Debernard, "Cooperative steering assist control system," in *2013 IEEE International Conference on Systems, Man, and Cybernetics, Manchester, UK*, 2013, pp. 941–946. https://doi.org/10.1109/SMC.2013.165

[4] C. Zhang, C. Zhuang, X. Zheng, R. Z. Cai, and M. Li, "Stochastic model predictive control approach to autonomous vehicle lane keeping," *J. Shanghai Jiaotong Univ. (Sci.)*, vol. 26, pp. 626–633, 2021. https://doi.org/10.1007/s12204-021-2352-y

[5] H. Imine and T. Madani, "Sliding-mode control for automated lane guidance of heavy vehicle," *Int. J. Robust Nonlinear Control*, vol. 23, no. 1, pp. 67–76, 2013. https://doi.org/10.1002/rnc.1818

[6] L. Li, F. Y. Wang, and Q. Z. Zhou, "An lmi approach to robust vehicle steering controller design," in *Proceedings of 2005 IEEE Intelligent Transportation Systems, Vienna, Austria*, 2005, pp. 90–95. https://doi.org/10.1109/ITSC.2005.1520075

[7] M. Netto, S. Chaib, and S. Mammar, "Lateral adaptive control for vehicle lane keeping," in *Proceedings of the 2004 American Control Conference, Boston, MA, USA*, 2004, pp. 2693–2698. https://doi.org/10.23919/ACC.2004.1383872

[8] Y. Jeong, "A personalized lane keeping system for autonomous vehicles based on RNN with temporal dependencies," *J. Mech Sci. Technol.*, vol. 36, no. 2, pp. 565–574, 2022. https://doi.org/10.1007/s12206-022-0105-y

[9] N. Basjaruddin, E. Rakhman, and F. Adinugraha, "Hardware simulation of lane keeping assist based on sensor fusion," *Int. J. Intell. Unmanned Syst.*, vol. 9, no. 3, pp. 192–203, 2020. https://doi.org/10.1108/IJIUS-04-2020-0005

[10] A. El Sallab, M. Abdou, E. Perot, and S. Yogamani, "End-to-end deep reinforcement learning for lane keeping assist," in *30th Conference on Neural Information Processing Systems (NIPS 2016), Barcelona, Spain*, 2016.

[11] R. Luo, D. W. Qian, and Q. C. Zhang, "Data-based reinforcement learning for lane keeping with input saturation," *Int. J. Adv. Mechatron. Syst.*, vol. 8, no. 1, pp. 9–15, 2020. https://doi.org/10.1504/IJAMECHS.2020.109897

[12] Q. Wang, W. C. Zhuang, L. M. Wang, and F. Ju, "Lane keeping assist for an autonomous vehicle based on deep reinforcement learning," in *WCX SAE World Congress Experience*, 2020. https://doi.org/10.4271/2020-01-0728

[13] M. Kim, J. Seo, M. Lee, and J. Choi, "Vision-based uncertainty-aware lane keeping strategy using deep reinforcement learning," *J. Dyn. Sys., Meas., Control*, vol. 143, no. 8, p. 084503, 2021. https://doi.org/10.1115/1.4050396

[14] W. S. Yang, Y. P. Chen, and Y. X. Su, "A double-layer mpc approach for collision-free lane tracking of on-road autonomous vehicles," *Actuators*, vol. 12, no. 4, p. 169, 2023. https://doi.org/10.3390/act12040169

[15] C. M. Wang and Y. C. Du, "Lane-changing strategy based on a novel sliding mode control approach for connected automated vehicles," *Appl. Sci.*, vol. 12, no. 21, p. 11000, 2022. https://doi.org/10.3390/app122111000

[16] R. H. Wang, J. B. Hu, and X. Q. Zhang, "Analysis of the driver's behavior characteristics in low volume freeway interchange," *Math. Probl. Eng.*, p. 2679516, 2016. https://doi.org/10.1155/2016/2679516

[17] R. He, H. P. Lv, S. Zhang, D. Zhang, and H. Zhang, "Lane following method based on improved DDPG algorithm," *Sensors (Basel)*, vol. 21, no. 14, p. 4827, 2021. https://doi.org/10.3390/s21144827

[18] W. Y. An, "Research on driver's lane change driving intention recognition method based on HMM," Ph.D. dissertation, Jilin University, 2020.

[19] X. R. Xie, G. S. Liu, Q. Cai, P. F. Wei, and H. Qu, "Multi-source sequential knowledge regression by using transfer RNN units," *Neural Netw.*, vol. 119, pp. 151–161, 2019.

[20] V. Leonhardt and G. Wanielik, "Recognition of lane change intentions fusing features of driving situation, driver behavior, and vehicle movement by means of neural networks," in *Advanced Microsystems for Automotive Applications*, 2017, pp. 59–69. https://doi.org/10.1007/978-3-319-66972-4_6

[21] E. T. Jeong and C. H. Lee, "A study on disturbance classification of unmanned vehicle data using SVM," *J. Control, Robot. Syst.*, vol. 28, no. 4, pp. 304–312, 2022. http://doi.org/10.5302/J.ICROS.2022.21.0190